THE JOURNAL OF PHYSICAL CHEMISTRY C

ARTICLE

pubs.acs.org/JPCC

Fluorine Treatment of TiO_2 for Enhancing Quantum Dot Sensitized Solar Cell Performance

Mahmoud Samadpour,[†,‡] Pablo P. Boix,[†] Sixto Giménez,[†] Azam Iraji Zad,[‡,§] Nima Taghavinia,[‡,§] Iván Mora-Seró,[*,†] and Juan Bisquert[†]

[†]Grup de Dispositius Fotovoltaics i Optoelectrònics, Departament de Física, Universitat Jaume I, 12071 Castelló, Spain

[‡]Institute for Nanoscience and Nanotechnology, Sharif University of Technology, P.O. Box 11155-8639, Tehran, Iran

[§]Department of Physics, Sharif University of Technology, P.O. Box 11155-9161, Tehran, Iran

Supporting Information

ABSTRACT: Surface treatments of TiO_2 nanostructure in semiconductor quantum dot sensitized solar cells (QDSCs) aimed to increase the photovoltaic conversion efficiencies of the solar cells are analyzed. A fluorine treatment, with NH_4F or HF, on the TiO_2 electrodes leads to a general increase of QDSCs performance in a range of QDSCs using different light absorbing materials: CdS, CdSe, and PbS/CdS. In contrast, no significant effect on QDSC performance has been observed after a $TiCl_4$ treatment conventionally used for high performance dye sensitized solar cells (DSCs). Surface and photoelectrochemical characterization of treated electrodes and full solar cells was carried out by means of X-ray photoelectron spectroscopy (XPS), impedance spectroscopy (IS), and applied bias voltage decay (ABVD), to understand the origin of the beneficial effect of fluorine. It was found that the origin of the enhancement is different depending on the semiconductor material (CdS, CdSe, and PbS/CdS). For CdS and CdSe, the recombination of photoinjected carrier is reduced after F treatment. On the other hand, for PbS/CdS, the treatment accelerates the deposition kinetics of PbS by successive ionic layer adsorption and reaction (SILAR), increasing the amount of deposited material and consequently the light harvesting. Our study indicates, in general, that treatments different from those conventionally used in DSCs are required and, specifically, that F treatment can be systematically used in QDSCs to increase the solar cell performance.

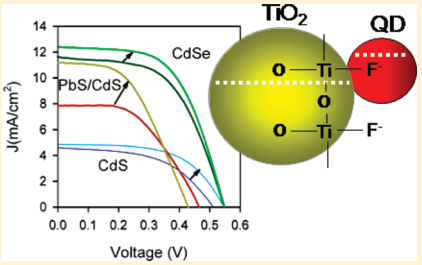

1. INTRODUCTION

In the past few years, semiconductor quantum dot sensitized solar cells (QDSCs) are receiving increasing attention.[1−5] Semiconductors possess high extinction coefficients and large intrinsic dipole moments.[6] In addition, their optoelectronic properties can be tailored at the nanoscale region. For example, band gap tunability by size (and shape) control (due to quantum confinement) provides an excellent tool for the design of light absorber materials.[7] Moreover, the observation of multiple exciton generation in colloidal QDs[8,9] has triggered the interest in semiconductor QDs as light harvesting materials. In spite of certain controversy,[10] very recently it has been demonstrated that internal quantum efficiencies higher than 100% in PbS nanocrystals are possible, provided that they are carefully coated on single crystal TiO_2 substrates.[11] Despite the novelty of the demonstration, the configuration employed has been extensively studied in dye sensitized solar cells (DSCs).[12] In DSCs, molecular dyes are used as light harvesting materials, injecting the photogenerated electrons into a nanostructured matrix of a wide band gap semiconductor (i.e., TiO_2) which subsequently transports the photogenerated electrons back to the contact electrode.[13] Dye molecules are regenerated by a redox couple in a proper electrolyte, which acts as the hole transporting media. In QDSCs, the molecular dyes are replaced by semiconductor materials generally showing a quantum confinement effect.[1]

Despite the formal analogy between QDSCs and DSCs, the fact that different light absorbing materials are used imposes a whole redesign of the QDSCs architecture in order to achieve higher conversion efficiencies. Replacing the light absorbing material must be carried out together with the substitution of the redox couple and electrolyte in order to maintain the absorber stability.[1,4,14] Additionally, the change of the electrolyte may impose a change of the counterelectrode material in order to minimize the potential drop at this interface.[15−18] On the other hand, the nanostructure of the wide band gap semiconductor (TiO_2) plays a significant role on the QDSC performance.[15,19−21] Consequently, a new design of QDSCs is compulsory, in order to increase the current power conversion efficiencies of 5%, using liquid electrolyte[21] or solid hole transporter.[22]

It has been shown that surface treatments play a dramatic role in QDSCs. They can be used to protect the semiconductor QDs[23,24] or to allow the control of recombination processes and band alignment, and, therefore, electron injection, in this

Received: March 25, 2011
Revised: May 24, 2011
Published: June 21, 2011

kind of cell.[1,4,14,15,25−28] ZnS[15,28] or SiO_2[26] coating increases significantly the efficiency of QDSCs, reducing the recombination and passivating the QD surfaces. The use of molecular dipoles permits the design of injection and recombination by the control of the band alignment in QDSCs.[24,25]

In this sense, the present study focuses on the specific design of the surface conditioning of the nanostructured TiO_2 matrix, prior to the deposition of QDs. During the manufacturing of DSCs, a $TiCl_4$ treatment on the transparent conductive oxide (TCO) prior to TiO_2 nanoparticle deposition and also after sintering of the TiO_2 nanoparticles is conventionally carried out.[29,30] The first $TiCl_4$ treatment aims at increasing the contact between TiO_2 nanoparticles and the conductive substrate, while the second treatment is responsible for a higher dye loading and a down-shift of the TiO_2 conduction band (CB) favoring the increase of photocurrent.[31] Particularly, this treatment is imperative when efficiencies higher than 11% are desired.[32−34]

Likewise, we have studied the effect of different treatments for the nanostructured TiO_2 electrodes, namely $TiCl_4$, NH_4F, and HF, on the photovoltaic performance of QDSCs. Fluorine treatments on TiO_2 have been previously reported, mainly in the domain of photocatalytic applications.[35−40] In the field of QDSCs, the group of Toyoda reported a significant increase of QDSCs efficiency, when a NH_4F treatment was applied on TiO_2 (before and after QD deposition).[41] In that study, an inverse opal TiO_2 architecture, and CdSe grown by chemical bath deposition, as light absorber, were used. Very recently, Lai and Chou reported an increase of solar performance after NH_4F treatment of a thin layer of TiO_2 for mesoporous metal oxide free CdSe solar cells.[42] In the present work, a systematic study for different semiconductor light absorbing materials [CdS, CdSe, and the combination of PbS and CdS (PbS/CdS)] is carried out. The different semiconductors were deposited on TiO_2 mesoporous electrodes by successive ionic layer adsorption and reaction (SILAR). The use of the SILAR method results in a high QDs loading on the TiO_2 surface. Consequently, high efficiency QDSCs can be produced.[43−47] We have observed that $TiCl_4$ treatment does not lead to any appreciable increase of the QDSCs efficiency, while both NH_4F and HF treatments produce an enhancement of the solar cell performance for all the analyzed light absorbing materials. Solar cells with and without the different surface treatments have been systematically analyzed in order to understand the origin of the beneficial effect of the fluorine treatment in QDSCs.

2. EXPERIMENTAL METHOD

Electrode Preparation. The photoanodes used in the present study are constituted by a double-layer of TiO_2 nanoparticles (transparent and opaque particles). The opaque layer, with enhanced light scattering, contains 300−400 nm TiO_2 particles (WER4-O Dyesol). The transparent layer is formed by either 20 nm TiO_2 nanoparticles (18NR-AO, Dyesol) or 37 nm TiO_2 nanoparticles (Ti-Nanoxide T37, Solaronix). The photoanodes were deposited by doctor blade on transparent conducting fluorine doped tin oxide (FTO) glass substrates (sheet resistance ∼10 Ω/□). The FTO coated glass was previously covered with a compact layer of TiO_2 deposited by spray pyrolysis of titanium-(IV) bis(acetoacetonato) di(isopropanoxylate). The resulting photoelectrodes were sintered at 450 °C, in order to achieve good electrical contact between the nanoparticles. The total thickness of the photoanodes was 14 ± 2 μm, measured with a profilometer Dektack 6 from Veeco.

Surface Treatments. The $TiCl_4$ treatment consisted of immersion of the as-sintered TiO_2 electrodes into a 0.04 M $TiCl_4$ solution for 30 min at 70 °C followed by calcination at 450 °C for 30 min. No $TiCl_4$ treatment on FTO, prior to the TiO_2 deposition, has been carried out. Two different fluorine treatments have been studied, employing NH_4F or HF. For the former one, a 1 M NH_4F solution was prepared by dissolving the NH_4F powder in Milli-Q water. For this fluorine treatment, the TiO_2 electrodes were soaked in the prepared solution for 5 min, unless other conditions are specified. After the fluorine treatment, the samples were rinsed with Milli-Q water for 1 min and dried with a nitrogen flow. For the later treatment, a 1 M hydrofluoridric acid solution was prepared by diluting 48% hydrofluoridric acid (Sigma Aldrich) with a solution of Milli-Q water and ethanol (1:1 in volume). The TiO_2 electrodes were soaked in the prepared HF acid solution for 5 min, only exposing the TiO_2 layer to the solution and protecting both FTO and glass with Scotch tape. After the fluorine treatment, the samples were rinsed in a solution of Milli-Q water and ethanol (1:1 in volume) for 1 min and then dried with a nitrogen flow.

Electrode Sensitization. Three different semiconductor absorbing materials have been employed: CdS, CdSe, and PbS/CdS. The semiconductors were *in situ* grown on the TiO_2 nanostructured electrodes by the SILAR methods recently described.[46,48,49] Briefly, for the deposition of CdS, two solutions with Cd and S precursors were prepared. Cd^{2+} ions have been deposited from a 0.05 M ethanolic solution of $Cd(NO_3)_2 \cdot 4H_2O$. The sulfide source was a 0.05 M solution of $Na_2S \cdot 9\ H_2O$ in methanol/water (50/50 v/v). A CdS coating in order to stabilize PbS[46,50] in PbS/CdS QDSCs was deposited using the same process. PbS QDs were deposited by SILAR on TiO_2 nanostructured electrodes following a procedure previously described.[50] The deposition of PbS QDs involves the use of two different solutions of metals and sulfide precursors. A 0.02 M methanolic solution of $Pb(NO_3)_2 \cdot 4H_2O$ was used as Pb^{2+} source and 0.02 M $Na_2S \cdot 9H_2O$ in methanol/water (50/50 v/v) was used as sulfide source. The CdS deposition is carried out immediately after PbS deposition. For CdSe sensitization, two solutions of 0.03 M $Cd(NO_3)_2$ dissolved in ethanol and another one containing the *in situ* generated 0.03 M Se^{2-} in ethanol were used; see ref 47 for more details. For sensitization, the electrodes were dipped successively in these solutions inside a glovebox under N_2 atmosphere.[43,45,47] A single SILAR cycle for CdS and PbS/CdS consisted of 1 min of dip-coating of the TiO_2 working electrode into the metal precursors (Pb^{2+} or Cd^{2+}) and subsequently into the sulfide solution, also for 1 min. A single SILAR cycle for CdSe consisted of 30 s of dip-coating of the TiO_2 working electrode into the Cd^{2+} precursor and subsequently into the selenide solution, for 30 s. After each precursor bath, the photoanode is thoroughly rinsed by immersion in the corresponding solvent to remove the chemical residuals from the surface and then dried with a N_2 gun. All the samples analyzed in this study have been coated with ZnS, after SILAR sensitization, by dipping alternately into 0.1 M $Zn(CH_3COO)_2$ and 0.1 M Na_2S solutions for 1 min/dip, rinsing with Milli-Q ultrapure water between dips. It has been shown that ZnS coating increases significantly the efficiency of QDSCs.[15,28] Two SILAR cycles were used for ZnS deposition.

Surface Characterization. The surface composition of TiO_2 and HF treated TiO_2 was studied by X-ray photoelectron spectroscopy (XPS) using an Al anode X-ray source. The base

Table 1. Average Photovoltaic Parameters of the QDSCs Tested under Standard Conditions (100 mW/cm^2, AM 1.5G): Photocurrent, j_{sc}, Open Circuit Voltage, V_{oc}, Fill Factor, FF, and Efficiency, η, Considering the Standard Deviation, as a Function of the Different Surface Treatments, TiO_2 Nanoparticle Size, and Semiconductor Light Harvesting Material[a]

sample	SILAR cycles	TiO_2 size (nm)	V_{oc} (mV)	J_{sc} (mA/cm^2)	FF	η (%)
TiO_2/CdS	5	37	515	4.36	0.53	1.19 ± 0.07
HF TiO_2/CdS	5	37	536	4.62	0.54	1.34 ± 0.05
NH_4F TiO_2/CdS	5	37	527	4.70	0.54	1.36 ± 0.15
NH_4F(30 min) TiO_2/CdS	5	37	529	4.17	0.56	1.255 ± 0.007
TiO_2/PbS/Cd	2/5	37	451	7.35	0.49	1.62 ± 0.19
NH_4F TiO_2/PbS/CdS	2/5	37	425	8.72	0.51	1.89 ± 0.02
HF TiO_2/PbS/CdS	2/5	37	434	10.09	0.48	2.1 ± 0.2
TiO_2/CdSe	7	37	557	11.35	0.45	2.84 ± 0.10
HF TiO_2/CdSe	7	37	564	12.50	0.51	3.64 ± 0.15
TiO_2/CdSe	7	20	534	12.34	0.53	3.49 ± 0.19
HF TiO_2/CdSe	7	20	545	12.05	0.57	3.7 ± 0.3
$TiCl_4$ TiO_2/CdSe	7	20	528	12.93	0.48	3.26 ± 0.10

[a] A complete summary, with the values for all the QDSCs analyzed, is provided in the Supporting Information S1.

pressure of the XPS chamber was below 1×10^{-9} Torr, and a concentric hemispherical analyzer (Specs model EA10 plus) was employed to measure the energy of emitted electrons from the surface of the sample.

QDSC Preparation. The solar cells were prepared by assembling the counterelectrode and a QD-sensitized electrode using a Scotch spacer (thickness 50 μm) and with a droplet (10 μL) of polysulfide electrolyte. The composition of the polysulfide electrolyte was 1 M Na_2S, 1 M S, and 0.1 M NaOH solution in Milli-Q ultrapure water. We have used Cu_2S counterelectrodes, clamping the sensitized electrode and the counterelectrode.[15,51] The Cu_2S counterelectrodes were prepared by immersing brass substrates into a HCl solution at 70 °C for 5 min and subsequently dipping into polysulfide solution for 10 min. This results in a porous Cu_2S electrode. The area of the cells was 0.24 cm^2. At least two cells were prepared at each different condition; a complete table with all the analyzed cells can be found in the Supporting Information.

Photoanode and Solar Cell Characterization. The optical absorption spectra of the photoanodes were recorded at 300−800 nm with a Cary 500 UV−vis Varian photospectroscometer. $J-V$ curves were obtained using a FRA equipped PGSTAT-30 from Autolab and a Keithley 2612 system source meter. $J-V$ measurements were carried out using a mask and no antireflective layer. Cells were illuminated using a solar simulator at AM1.5 G, where the light intensity was adjusted with an NREL calibrated Si solar cell with a KG-5 filter to one sun intensity (100 mW/cm^2). Incident photon to electron conversion efficiency (IPCE) measurements have been performed employing a 150 W Xe lamp coupled with a computer-controlled monochromator; the photocurrent was measured using an amperometer 70310 from Oriel Instruments. Impedance spectroscopy (IS) measurement and applied bias voltage decay (ABVD)[52] were carried out with a FRA equipped PGSTAT-30 from Autolab. IS measurements were carried out by applying a 20 mV ac signal and scanning in a frequency range between 400 kHz and 0.1 Hz, at different forward applied bias.

3. RESULTS AND DISCUSSION

In order to determine the effect of the different surface treatments, $TiCl_4$, NH_4F, and HF, on the photovoltaic performance of full solar cell devices, several samples have been prepared at each condition. Table 1 shows the average solar cell parameters obtained for these QDSCs (photocurrent, j_{sc}, open circuit voltage, V_{oc}, fill factor, FF, and efficiency, η), with the standard deviation, as a function of the different surface treatments, TiO_2 nanoparticle size, and semiconductor light harvesting material, tested under standard conditions (100 mW/cm^2, AM 1.5G). All samples have been tested using polysulfide as electrolyte and Cu_2S as counterelectrode.

The effect of the $TiCl_4$ treatment was evaluated on CdSe QDSCs. No increase in the average efficiency of $TiCl_4$ treated cells was observed (see Table 1). Indeed, a small decrease in efficiency due to the reduction of the average V_{oc} and FF was obtained. This result clearly reflects that the $TiCl_4$ treatment does not have a beneficial effect on QDSCs using TiO_2 nanoparticles, conversely to that reported for DSCs. However, it has been recently reported that the $TiCl_4$ treatment has a remarkable effect on QDSCs based on SnO_2 spheres acting as electron conducting media.[53]

On the other hand, a systematic beneficial effect is observed for fluorine treated photoanodes for the three different sensitizers tested: CdS, CdSe, and PbS/CdS (see Table 1). The effectiveness of the fluorine treatment decreases when the soaking time is extended from 5 to 30 min (see Table 1). Both treatments, HF and NH_4F solutions, for TiO_2 surface fluorination produce an enhancement on QDSC performance, observing the same mechanism for improvement of solar cells efficiency. To analyze the surface modification of TiO_2 by this treatment, fluorine treated TiO_2 electrodes were analyzed by XPS, in the case of HF treatment. Figure 1 shows the XPS spectra of TiO_2 samples before and after HF treatment. For HF treated TiO_2, a F 1s peak at 684.6 eV was observed (Figure 1a), which can be attributed either to F^- grafted on the surface of TiO_2 by substitution of the surface hydroxyl groups or to physisorbed F^-. It is known that the binding energy of the fluorine incorporated into the TiO_2 lattice is higher compared to that of F^- grafted on the surface.[35,38] Since no additional peaks were identified at higher energies, the detected F^- should correspond to grafted F^-. Further validation of this assumption was carried out by investigating the high-resolution O 1s core level of bare and HF treated TiO_2 samples. The XPS spectrum for O 1s is asymmetric,

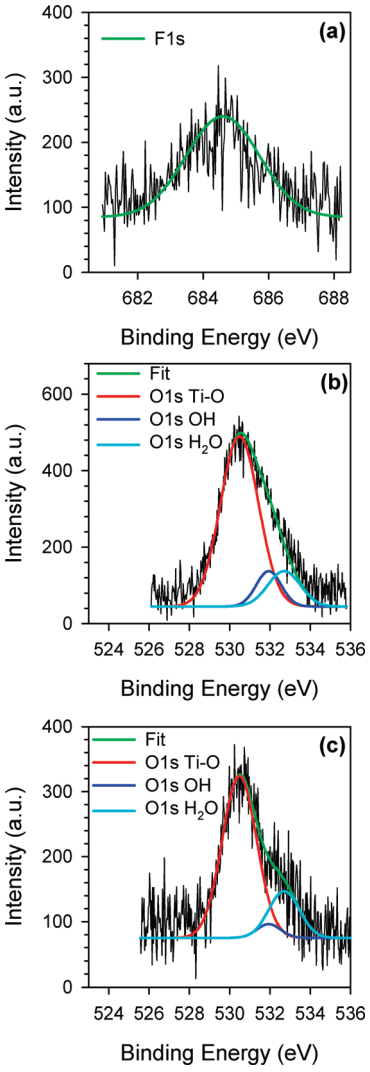

Figure 1. XPS spectra of the bare and HF treated TiO_2: F 1s high resolution spectra in HF treated TiO_2 (a); O 1s region for the bare (b) and HF treated (c) TiO_2.

which arises from the presence of different chemical compositions for the oxygen. The main contribution is related to Ti−O bonds with a XPS peak at 530.49 eV. The other peaks originate from the oxygen at the surface OH^- groups (531.94 eV) and adsorbed H_2O with a peak at around 532.7 eV.[54] Accordingly, the XPS spectra of Figure 1b and c have been fitted using the convolution of three Gaussian peaks (O 1s from Ti−O, OH, and H_2O). The relative intensities of the fitted peaks for TiO_2 and HF treated TiO_2, for the O 1s region, are summarized in Table 2. It can be seen that the contribution of O 1s (OH^-) is decreased from 10.3% to 4.5% after the HF treatment. This decrease reveals that F^- ions are replacing some OH^- groups at the TiO_2 surface. The Ti−F bond can be easily formed through the following reaction:

$$Ti{-}OH + F^- \rightarrow Ti{-}F + OH^- \quad (1)$$

The fraction of Ti−O bonds was almost identical for bare and treated samples (Table 2), also confirming that there is no incorporation of F^- into the TiO_2 lattice. Finally, the increase

Table 2. Relative Intensity of the Three Fitted XPS Peaks for TiO_2 and HF Treated TiO_2, in the O 1s Region (Figure 1b and c)

sample	O 1s Ti−O (%)	O 1s O−H (%)	O 1s H_2O (%)
TiO_2	76.2	10.3	13.5
HF TiO_2	76	4.5	19.5

of the O 1s (H_2O) fraction from 13.5% to 19.5% is related to more adsorbed H_2O on the surface after treatment with an aqueous solution of HF acid. This analysis confirms that the TiO_2 surface is modified after fluorine treatment.

Parameters such as the concentration of fluorine solution and, particularly, the pH influence the TiO_2 photocatalytic properties by changing the amount of the surface fluorination. According to previously reported results, the Ti−F bond on the surface remains the dominant species in the acidic pH range.[39,40] The study of the reversibility of fluorination (back-exchange of F^- with OH^-) by treating the TiO_2−F samples with NaOH solutions at increasing pH shows that no back-exchange was obtained until pH = 12.0 was reached.[39] We measured the pH of the ammonium fluoride solution that we used for treating our samples, and it was 5.8, which is an acidic pH and ensures the effective surface fluorination.[39,40] Also, after fluorine treatment, samples were put in a solution of Milli-Q water for 1 min and then dried with a nitrogen flow. Regarding the pH of Milli-Q water (almost 7), the back-exchange of F^- with OH^- is not expected to happen at this pH.[39] In this sense, removal of F^- is not expected on the TiO_2 surface after rinsing.[36]

As shown in Table 1, fluorine surface modification produces a systematic enhancement of QDSCs performance. Representative examples of $J-V$ curves obtained for CdS, CdSe, and PbS/CdS QDSCs are plotted in Figure 2c, f, and i, respectively. There is certain dispersion in the results observed for solar cells identically prepared (see Figure 2i and the Supporting Information), which can be mainly attributed to the scattering in electrode thickness, but a clear trend is observed in spite of this dispersion. Comparing treated and untreated TiO_2 electrodes, no significant change in the QD loading is observed by reflectance measurement for CdS and CdSe sensitized electrodes (see Figure 2a and d). Conversely, a clear decrease of reflectance is observed for PbS/CdS electrodes at long wavelengths (above 500 nm; see Figure 2g). The shift of the absorption threshold to longer wavelengths has been previously observed as the number of PbS SILAR cycles increases, and it correlates to the growth of the PbS QDs.[50] Consequently, a higher PbS loading is obtained after the fluorine treatment, despite the same number of SILAR cycles being performed for treated and untreated samples. This fact indicates a change in the reaction kinetics of the PbS deposition process by SILAR. We are currently studying this point. The fluorine attached to the TiO_2 surface produces an acidification of the surface that probably enhances the dissociation of $Pb(NO_3)_2$, consequently increasing the deposition rate.

IPCE measurements are plotted in Figure 2b, e, and h, shown as a slight increase of current efficiency at longer wavelengths. This increase is particularly significant for PbS/CdS cells, is in good agreement with reflectance measurements, and explains the higher photocurrents observed for fluorine treated PbS/CdS cells (see Figure 2i). Conversely, very similar reflectance and IPCE spectra have been obtained for both treated and untreated CdS and CdSe QDSCs. Then, the origin of the beneficial effect of fluorine treatment on these solar cells must be sought elsewhere.

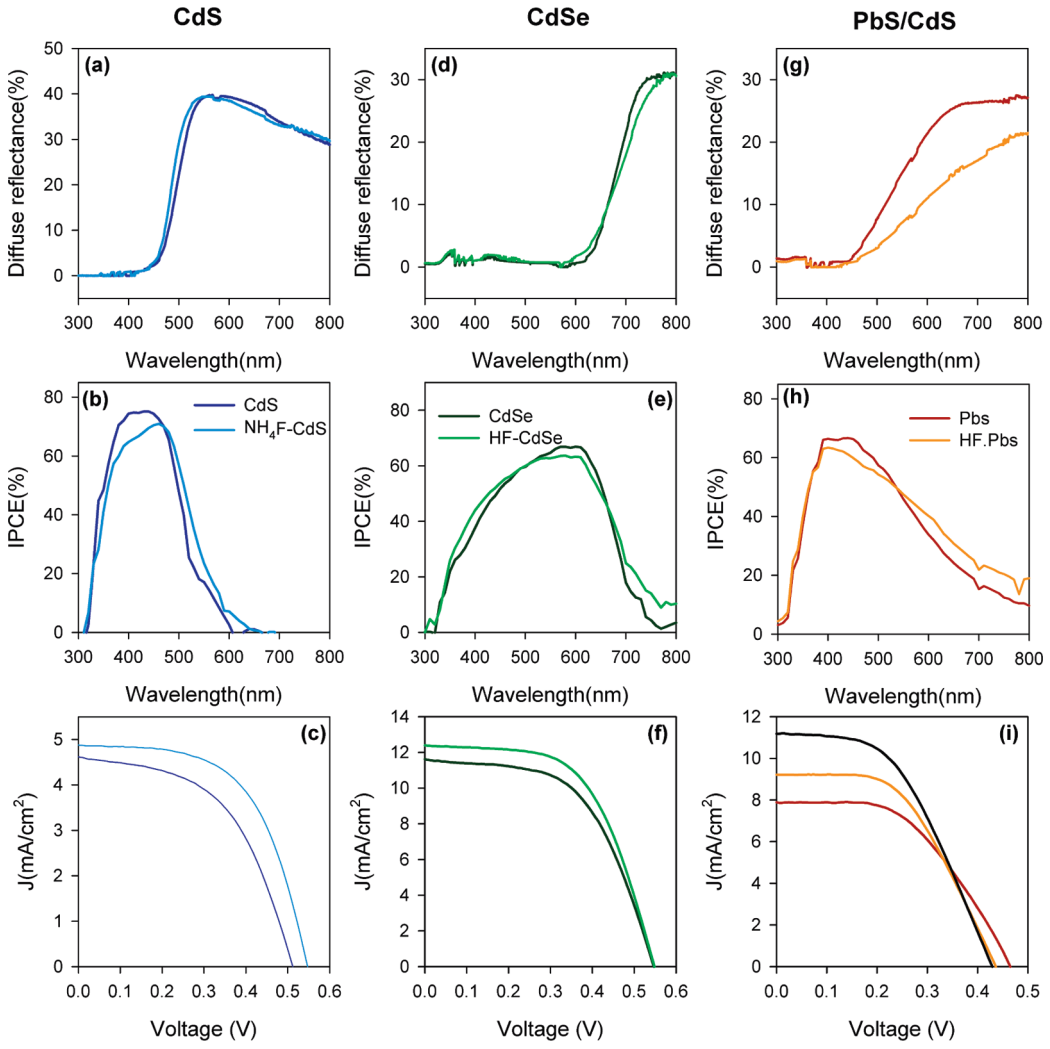

Figure 2. Diffuse reflectance, IPCE, and $J-V$ curves for fluorine treated and untreated QDSCs. CdS QDSCs (a) diffuse reflectance, (b) IPCE, and (c) $J-V$ curves. CdSe QDSCs (d) diffuse reflectance, (e) IPCE, and (f) $J-V$ curves. PbS/CdS QDSCs (g) diffuse reflectance, (h) IPCE, and (i) $J-V$ curves. The black line represents an identically treated sample showing the dispersion between cells. The exact photovoltaic parameters of the solar cells represented in these plots can be found in the Supporting Information.

For this purpose, impedance spectroscopy and applied bias voltage decay measurements were carried out on QDSCs. The chemical capacitance, C_μ (Figure 3a, d, and g), and recombination resistance, R_{rec} (Figure 3b, e, and h), have been extracted from IS measurements using the previously developed model.[43,55,56] Impedance characterization allows separation of the effect of each part of the photovoltaic device, as sensitized electrode, counterelectrode, diffusion in the electrolyte, and series resistance at each applied voltage bias, V_{app}.[56] In Figure 3, C_μ is plotted against the voltage drop at the sensitized electrode, V_F, removing the voltage drop of series resistance, V_{series} (contacts, counterelectrode, electrolyte diffusion), by $V_F = V_{app} - V_{series}$. The slope of C_μ reflects the TiO_2 density of states; consequently, a shift in the chemical capacitance (as observed in Figure 3d and g) indicates a displacement of the TiO_2 conduction band edge.[56] In the case of CdSe QDSCs, a downward movement of TiO_2 CB is observed, while for PbS/CdS an upward displacement is obtained.

The recombination process can be analyzed by the recombination resistance, as this resistance is proportional to the inverse of the recombination rate. But to evaluate properly the recombination resistances of different cells, they have to be compared under the same conditions of electron density in TiO_2, n, as the recombination rate is proportional to n. V_F is proportional to the rise of the Fermi level of electrons in TiO_2, $V_F = (E_{Fn} - E_{F0})/q$, where q is the positive elementary charge and E_{Fn} and E_{F0} are the electron Fermi level and the electron Fermi level at equilibrium, respectively. To analyze the recombination resistance, R_{rec}, on the basis of a similar number of electrons (i.e., the same distance between the electron Fermi level, E_{Fn}, and the conduction band (CB) of TiO_2, E_{CB}), the shift of CB has been corrected in Figure 3e and h, where the voltage scale is the voltage drop in a common equivalent conduction band (CB), V_{ecb}, where the effect of the different TiO_2 CBs between samples is removed. The criterion for the modified scale is to shift the chemical capacitances of the analyzed samples until they overlap. The same shift applied to the chemical capacitance, in order to attain the overlap, has been applied to R_{rec} to obtain the R_{rec} vs V_{ecb} plot. In this representation, the effect of the different TiO_2 CBs between samples is removed. The methods to obtain the dependences

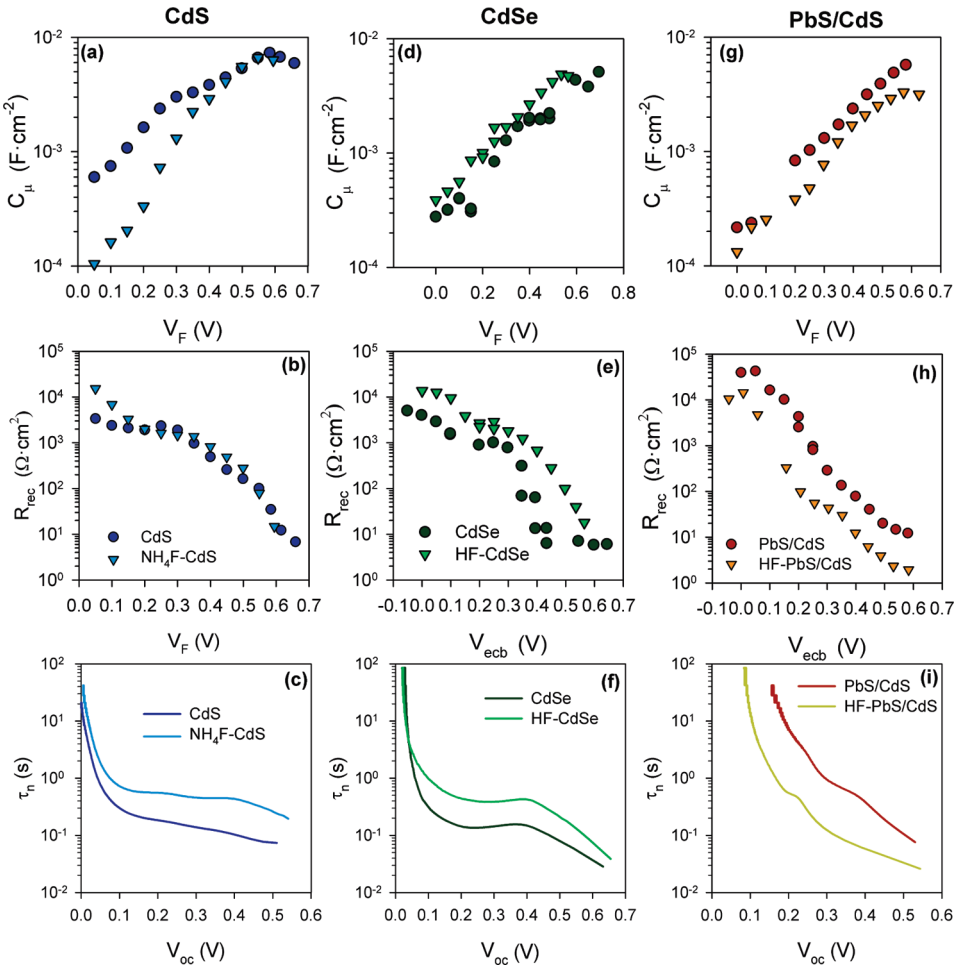

Figure 3. Chemical capacitance, recombination resistance, and electron lifetime for fluorine treated and untreated QDSCs. CdS QDSCs (a) chemical capacitance, (b) recombination resistance, and (c) electron lifetime. CdSe QDSCs (d) chemical capacitance, (e) recombination resistance, and (f) electron lifetime. PbS/CdS QDSCs (g) chemical capacitance, (h) recombination resistance, and (i) electron lifetime. Chemical capacitance and recombination resistance were obtained from IS measurements, while electron lifetime was obtained from ABVD measurements.

against V_F and V_{ecb} from IS measurements have been previously reported,[25,43,50] and they are extensively reviewed in a recent paper.[56]

Regarding PbS/CdS QDSCs, an upward shift of the TiO_2 CB takes place on fluorine treated samples, as derived from the capacitance measurements (Figure 3g). After correcting this shift, the fluorine treated samples exhibit lower recombination resistance (higher recombination) compared to their untreated counterparts (Figure 3h). These two trends are in excellent agreement with the increase of PbS loading (Figure 2g), as has been previously reported when comparing samples with different numbers of PbS SILAR cycles.[50] Therefore, the enhanced performance of PbS/CdS QDSCs after fluorine treatment can be attributed to faster PbS deposition kinetics, as has been previously noted. This higher PbS loading leads to higher light harvesting and concomitantly higher j_{sc}, while the lower R_{rec} explains the reduced V_{oc} (see Figure 2i and Table 1).

On the other hand, the fluorine treatment does not affect the deposition reaction kinetics for CdS and CdSe QDSCs, since the same amount of light harvesting material is obtained for both treated and untreated samples (Figure 2a and d). However, higher recombination resistance is measured on fluorine treated samples, particularly for CdSe QDSCs (Figure 3e). The surface Ti−F group seems to act as an electron-trapping site slowing down the interfacial electron transfer rates by tightly holding trapped electrons due to the strong electronegativity of fluorine.[36]

The slower recombination extracted from IS for CdS and CdSe QDSCs has been further confirmed by comparing the electron lifetimes, τ_n, of fluorine treated and untreated samples (Figure 3c and f). τ_n has been measured by applied bias voltage decay (ABVD).[52] Consistently, shorter lifetimes are obtained for fluorine treated PbS/CdS cells (Figure 3i), as expected from the lower recombination resistance measured.

4. CONCLUSIONS

We have shown that the $TiCl_4$ treatment, conventionally used in DSCs, did not offer any improvement for the QDSCs tested. Conversely, fluorine treatments, either with NH_4F or HF, on TiO_2 nanostructured electrodes have a general beneficial effect on the QDSCs efficiency, using CdS, CdSe, and PbS/CdS QDs directly grown on the TiO_2 electrodes by SILAR. The reason for the increase of efficiency observed after the fluorine treatment depends on the semiconductor light absorbing material. The faster deposition reaction kinetics of PbS leads to a higher amount of light harvesting material in PbS/CdS QDSCs. In

dx.doi.org/10.1021/jp202819y |J. Phys. Chem. C 2011, 115, 14400–14407

contrast, the decrease of recombination rate is responsible for the improved efficiency in CdS and CdSe QDSCs, as evidenced by IS and ABVD measurements. After the fluorine treatment, efficiencies as high as 1.54%, 2.36%, and 3.93% have been obtained for CdS, PbS/CdS, and CdSe QDSCs, respectively (see the Supporting Information). Two important conclusions, one practical and another one more general, can be extracted from the present study: First, the fluorine treatments can be systematically used to enhance the efficiency of QDSCs, as $TiCl_4$ is used with the same purpose in DSCs. On the other hand, in order to improve the efficiency of QDSCs, a specific design of the device architecture, taking into account the particular characteristics of semiconductor QDs, is compulsory.

■ ASSOCIATED CONTENT

Supporting Information. Complete list of analyzed cells. This material is available free of charge via the Internet at http://pubs.acs.org.

■ AUTHOR INFORMATION

Corresponding Author
*E-mail: sero@fca.uji.es.

■ ACKNOWLEDGMENT

This work was partially supported by the Ministerio de Educación y Ciencia of Spain under Projects HOPE CSD2007-00007 (Consolider-Ingenio 2010), JES-NANOSOLAR PLE2009-0042, and MAT 2010-19827 and by Generalitat Valenciana Project PROMETEO/2009/058.

■ REFERENCES

(1) Hodes, G. *J. Phys. Chem. C* **2008**, *112*, 17778–17787.
(2) Kamat, P. V. *J. Phys. Chem. C* **2008**, *112*, 18737–18753.
(3) Kamat, P. V.; Tvrdy, K.; Baker, D. R.; Radich, J. G. *Chem. Rev.* **2010**, *110*, 6664–6688.
(4) Mora-Seró, I.; Bisquert, J. *J. Phys. Chem. Lett.* **2010**, *1*, 3046–3052.
(5) Rühle, S.; Shalom, M.; Zaban, A. *ChemPhysChem.* **2010**, *11*, 2290–2304.
(6) Yu, W.; Qu, L. H.; Guo, W. Z.; Peng, X. G. *Chem. Mater.* **2003**, *15*, 2854–2860.
(7) Alivisatos, A. P. *Science* **1996**, *271*, 933–937.
(8) Ellingson, R. J.; Beard, M. C.; Johnson, J. C.; Yu, P.; Micic, O. I.; Nozik, A. J.; Shabaev, A.; Efros, A. L. *Nano Lett.* **2005**, *5*, 865–871.
(9) Schaller, R. D.; Klimov, V. I. *Phys. Rev. Lett.* **2004**, *92*, 186601.
(10) Trinh, M. T.; Houtepen, A. J.; Schins, J. M.; Hanrath, T.; Piris, J.; Knulst, W.; Goossens, A. P. L. M.; Siebbeles, L. D. A. *Nano Lett.* **2008**, *8*, 1713–1718.
(11) Sambur, J. B.; Novet, T.; Parkinson, B. A. *Science* **2010**, *330*, 63–66.
(12) O'Regan, B.; Gratzel, M. *Nature* **1991**, *353*, 737–740.
(13) Bisquert, J.; Cahen, D.; Hodes, G.; Rühle, S.; Zaban, A. *J. Phys. Chem. B* **2004**, *108*, 8106–8118.
(14) Mora-Seró, I.; Giménez, S.; Fabregat-Santiago, F.; Gómez, R.; Shen, Q.; Toyoda, T.; Bisquert, J. *Acc. Chem. Res.* **2009**, *42*, 1848–1857.
(15) Giménez, S.; Mora-Seró, I.; Macor, L.; Guijarro, N.; Lana-Villarreal, T.; Gómez, R.; Diguna, L. J.; Shen, Q.; Toyoda, T.; Bisquert, J. *Nanotechnology* **2009**, *20*, 295204.
(16) Tachan, Z.; Shalom, M.; Hod, I.; Rühle, S.; Tirosh, S.; Zaban, A. *J. Phys. Chem. C* **2011**, *115*, 6162–6166.
(17) Yang, Z.; Chen, C.-Y.; Liu, C.-W.; Li, C.-L.; Chang, H.-T. *Adv. Energy Mater.* **2011**, *1*, 259–264.
(18) Deng, M.; Huang, S.; Zhang, Q.; Li, D.; Luo, Y.; Shen, Q.; Toyoda, T.; Meng, Q. *Chem. Lett.* **2010**, *39*, 1168–1170.
(19) Baker, D. R.; Kamat, P. V. *Adv. Funct. Mater.* **2009**, *19*, 805–811.
(20) Kongkanand, A.; Tvrdy, K.; Takechi, K.; Kuno, M.; Kamat, P. V. *J. Am. Chem. Soc.* **2008**, *130*, 4007–4015.
(21) Zhang, Q.; Guo, X.; Huang, X.; Huang, S.; Li, D.; Luo, Y.; Shen, Q.; Toyoda, T.; Meng, Q. *Phys. Chem. Chem. Phys.* **2011**, *13*, 4659–4667.
(22) Chang, J. A.; Rhee, J. H.; Im, S. H.; Lee, Y. H.; Kim, H.-J.; Seok, S. I.; Nazeeruddin, M. K.; Grätzel, M. *Nano Lett.* **2010**, *10*, 2609–2612.
(23) Shalom, M.; Albero, J.; Tachan, Z.; Martínez-Ferrero, E.; Zaban, A.; Palomares, E. *J. Phys. Chem. Lett.* **2010**, *1*, 1134–1138.
(24) Shalom, M.; Dor, S.; Rühle, S.; Grinis, L.; Zaban, A. *J. Phys. Chem. C* **2009**, *113*, 3895–3898.
(25) Barea, E. M.; Shalom, M.; Giménez, S.; Hod, I.; Mora-Seró, I.; Zaban, A.; Bisquert, J. *J. Am. Chem. Soc.* **2010**, *132*, 6834–6839.
(26) Liu, Z.; Miyauchi, M.; Uemura, Y.; Cui, Y.; Hara, K.; Zhao, Z.; Sunahara, K.; Furube, A. *Appl. Phys. Lett.* **2010**, *96*, 233107.
(27) Shalom, M.; Rühle, S.; Hod, I.; Yahav, S.; Zaban, A. *J. Am. Chem. Soc.* **2009**, *131*, 9876–9877.
(28) Shen, Q.; Kobayashi, J.; Diguna, L. J.; Toyoda, T. *J. Appl. Phys.* **2008**, *103*, 084304.
(29) Kambe, S.; Nakade, S.; Wada, Y.; Kitamura, T.; Yanagida, S. *J. Mater. Chem.* 2002, *12*, 723−728.
(30) Wang, P.; Zakeeruddin, S. M.; Comte, P.; Charvet, R.; Humphry-Baker, R.; Grätzel, M. *J. Phys. Chem. B* **2003**, *107*, 14336–14341.
(31) Sommeling, P. M.; O'Regan, B. C.; Haswell, R. R.; Smit, H. J. P.; Bakker, N. J.; Smits, J. J. T.; Kroon, J. M.; van Roosmalen, J. A. M. *J. Phys. Chem. B* **2006**, *110*, 19191–19197.
(32) Cao, Y.; Bai, Y.; Yu, Q.; Cheng, Y.; Liu, S.; Shi, D.; Gao, F.; Wang, P. *J. Phys. Chem. C* **2009**, *113*, 6290–6297.
(33) Gao, F.; Wang, Y.; Shi, D.; Zhang, J.; Wang, M.; Jing, X.; Humphry-Baker, R.; Wang, P.; Zakeeruddin, S. M.; Grätzel, M. *J. Am. Chem. Soc.* **2008**, *130*, 10720–10728.
(34) Yu, Q.; Wang, Y.; Yi, Z.; Zu, N.; Zhang, J.; Zhang, M.; Wang, P. *ACS Nano* **2010**, *4*, 6032–6038.
(35) Li, D.; Haneda, H.; Hishita, S.; Ohashi, N.; Labhsetwar, N. K. *J. Fluorine Chem.* **2005**, 126.
(36) Park, H.; Choi, W. *J. Phys. Chem. B* **2004**, *108*, 4086–4093.
(37) Wang, C. M.; Mallouk, T. E. *J. Phys. Chem.* **1990**, *94*, 423–428.
(38) Yu, J. C.; Yu, J.; Ho, W.; Jiang, Z.; Zhang, L. *Chem. Mater.* **2002**, *14*, 3808–3816.
(39) Minella, M.; Faga, M. G.; Maurino, V.; Minero, C.; Pelizzetti, E.; Coluccia, S.; Martra, G. *Langmuir* **2010**, *26*, 2521–2527.
(40) Minero, C.; Mariella, G.; Maurino, G.; Pelizzetti, E. *Langmuir* **2000**, *16*, 2632–2641.
(41) Diguna, L. J.; Shen, Q.; Kobayashi, J.; Toyoda, T. *Appl. Phys. Lett.* **2007**, *91*, 023116.
(42) Lai, C.-H.; Chou, P.-T. *Chem. Commun.* **2011**, *47*, 3448–3450.
(43) Gónzalez-Pedro, V.; Xu, X.; Mora-Seró, I.; Bisquert, J. *ACS Nano* **2010**, *4*, 5783–5790.
(44) Guijarro, N.; Lana-Villarreal, T.; Shen, Q.; Toyoda, T.; Gómez, R. *J. Phys. Chem. C* **2010**, *114*, 21928–21937.
(45) Lee, H. J.; Bang, J.; Park, J.; Kim, S.; Park, S.-M. *Chem. Mater.* **2010**, *22*, 5636–5643.
(46) Lee, H. J.; Leventis, H. C.; Moon, S.-J.; Chen, P.; Ito, S.; Haque, S. A.; Torres, T.; Nüesch, F.; Geiger, T.; Zakeeruddin, S. M.; Grätzel, M.; Nazeeruddin, M. K. *Adv. Funct. Mater.* **2009**, *19*, 2735–2742.
(47) Lee, H. J.; Wang, M.; Chen, P.; Gamelin, D. R.; Zakeeruddin, S. M.; Grätzel, M.; Nazeeruddin, M. K. *Nano Lett.* **2009**, *9*, 4221–4227.
(48) Chang, C.-H.; Lee, Y.-L. *Appl. Phys. Lett.* **2007**, *91*, 053503.
(49) Lee, H. J.; Chen, P.; Moon, S.-J.; Sauvage, F.; Sivula, K.; Bessho, T.; Gamelin, D. R.; Comte, P.; Zakeeruddin, S. M.; Seok, S. I.; Grätzel, M.; Nazeeruddin, M. K. *Langmuir* **2009**, *25*, 7602–7608.
(50) Braga, A.; Giménez, S.; Concina, I.; Vomiero, A.; Mora-Seró, I. *J. Phys. Chem. Lett.* **2011**, *2*, 454–460.
(51) Hodes, G.; Manassen, J.; Cahen, D. *J. Electrochem. Soc.* **1980**, *127*, 544–549.

(52) Bisquert, J.; Zaban, A.; Greenshtein, M.; Mora-Seró, I. *J. Am. Chem. Soc.* **2004**, *126*, 13550–13559.
(53) Hossain, M. A.; Yang, G.; Parameswaran, M.; Jennings, J. R.; Wang, Q. *J. Phys. Chem. C* **2010**, *114*, 21878–21884.
(54) Pouilleau, J.; Devilliers, D.; Garrido, F.; Durand-Vidal, S.; Mahé, E. *Mater. Sci. Eng., B* **1997**, *47*, 235–243.
(55) Fabregat-Santiago, F.; Bisquert, J.; Garcia-Belmonte, G.; Boschloo, G.; Hagfeldt, A. *Sol. Energy Mater. Sol. Cells* **2005**, *87*, 117–131.
(56) Fabregat-Santiago, F.; Garcia-Belmonte, G.; Mora-Seró, I.; Bisquert, J. *Phys. Chem. Chem. Phys.* **2011**, *13*, 9083–9118.